




# Tumor cell SYK expression modulates the tumor immune microenvironment composition in human cancer via TNF- $\alpha$ dependent signaling

Adam Aguirre-Ducler,<sup>1,2</sup> Nicole Gianino,<sup>1</sup> Franz Villarroel-Espindola <sup>1</sup>,  
Shruti Desai <sup>1</sup>, Daiwei Tang,<sup>3</sup> Hongyu Zhao,<sup>3</sup> Konstantinos Syrigos,<sup>4</sup>  
William L Trepicchio,<sup>5</sup> Karuppiah Kannan,<sup>5</sup> Richard C Gregory,<sup>5</sup>  
Kurt A Schalper <sup>1</sup>

**To cite:** Aguirre-Ducler A, Gianino N, Villarroel-Espindola F, *et al.* Tumor cell SYK expression modulates the tumor immune microenvironment composition in human cancer via TNF- $\alpha$  dependent signaling. *Journal for ImmunoTherapy of Cancer* 2022;**10**:e005113. doi:10.1136/jitc-2022-005113

► Additional supplemental material is published online only. To view, please visit the journal online (<http://dx.doi.org/10.1136/jitc-2022-005113>).

Accepted 01 July 2022



© Author(s) (or their employer(s)) 2022. Re-use permitted under CC BY-NC. No commercial re-use. See rights and permissions. Published by BMJ.

For numbered affiliations see end of article.

## Correspondence to

Dr Kurt A Schalper;  
kurt.schalper@yale.edu

## ABSTRACT

**Background** The expression of SYK in cancer cells has been associated with both tumor promoting and tumor suppressive effects. Despite being proposed as anticancer therapeutic target, the possible role of SYK in modulating local adaptive antitumor immune responses remains uncertain. Using detailed analysis of primary human tumors and in vitro models, we reveal the immunomodulatory effect of SYK protein in human solid cancer.

**Methods** We spatially mapped SYK kinase in tumor cells, stromal cells and tumor-infiltrating leukocytes (TILs) in 808 primary non-small cell lung carcinomas (NSCLCs) from two cohorts and in 374 breast carcinomas (BCs) from two independent cohorts. We established the associations of localized SYK with clinicopathologic variables and outcomes. The immunomodulatory role of SYK on tumor cells was assessed using in vitro cytokine stimulation, transcriptomic analysis and selective SYK blockade using a small molecule inhibitor. Functional responses were assessed using cocultures of tumor cells with peripheral blood lymphocytes. T cell responses in baseline and post-treatment biopsies from patients with BC treated with a SYK inhibitor in a phase I clinical trial were also studied.

**Results** Elevated tumor cell or leukocyte SYK expression was associated with high CD4<sup>+</sup> and CD8<sup>+</sup> TILs and better outcome in both NSCLC and BC. Tumor cell SYK was associated with oncogenic driver mutations in EGFR or KRAS in lung adenocarcinomas and with triple negative phenotype in BC. In cultured tumor cells, SYK was upregulated by TNF $\alpha$  and required for the TNF $\alpha$ -induced proinflammatory responses and T cell activation. SYK blockade after nivolumab in a phase I clinical trial including three patients with advanced triple negative BC reduced TILs and T cell proliferation. Our work establishes the proinflammatory function of tumor cell SYK in lung and breast cancer. SYK signaling in cultured tumor cells is required for T cell activation and SYK blockade limits adaptive antitumor immune responses and tumor rejection in patients with cancer.

**Conclusions** Together, our results establish the immunomodulatory role of SYK expression in human solid tumors. This information could be used to develop novel biomarkers and/or therapeutic strategies.

## BACKGROUND

Spleen tyrosine kinase (SYK) is a 72 kDa cytoplasmic non-receptor protein tyrosine kinase and one of the two members of the SYK family (SYK and ZAP-70). It is primarily expressed in hematopoietic cells including B-lymphocytes, mast cells, macrophages, neutrophils and myeloid-derived suppressor cells.<sup>1</sup> In immune cells, SYK has essential functions in cell proliferation, differentiation and phagocytosis.<sup>2,3</sup> SYK can also be expressed in non-immune cells including endothelial and epithelial cells, fibroblasts, neurons,<sup>4</sup> as well as in tumor cells/tissues.<sup>5</sup>

Cellular fractionation and immunofluorescence studies have revealed that SYK can be located in both the nuclear and cytoplasmic cell compartment.<sup>6</sup> Transcription of the SYK gene produces two alternatively spliced transcripts: the full-length SYK(L) and a shorter form SYK(S) lacking 23 residues within the interdomain B segment. The interdomain B contains a nuclear localization signal required for the nuclear expression.<sup>7</sup> SYK(L) is present in both the cytoplasm and nucleus, whereas SYK(S) allocates only to the cytoplasm and maintains the major structural domains (two tandem Src homology-2 domains and a kinase domain).

SYK is rarely mutated in cancer and the effect of SYK signaling activation may be cell-type dependent.<sup>8</sup> There are considerable data supporting a role for SYK in hematologic malignancies, and it is a prominent mediator of tonic and chronic signaling through the BCR in multiple B cell lymphomas where it supports cell survival.<sup>5,9</sup> The role of SYK in solid tumors is less clear, and studies in melanoma, breast and gastric carcinomas support a tumor suppressive effect.<sup>10–12</sup> In contrast,

human gliomas express a SYK signaling network associated with tumor progression, and SYK inhibition reduces invasion and cell migration and alters the immune composition of gliomas in syngeneic mice.<sup>13</sup> A recent study found that SYK inhibition reduced tumor growth/metastases and increased the levels of proinflammatory cytokines and CD8<sup>+</sup> T cell responses in lung and melanoma mouse models, supporting a possible role as immunostimulatory anticancer agent.<sup>14</sup>

Here, we studied the immunomodulatory role and clinical significance of SYK in human non-small cell lung carcinomas (NSCLCs) and breast carcinomas (BCs) using direct tissue analysis and *in vitro* models. Our results reveal a prominent association between tumor cell SYK expression and favorable adaptive antitumor immune responses. SYK expression in tumor cells is induced by TNF $\alpha$  and required for the TNF $\alpha$ -induced proinflammatory responses. Consistent with this, SYK blockade reduces TILs and T cell proliferation in patients with advanced triple negative breast cancer (TNBC). Together, our results reveal a novel immunomodulatory role of SYK expression in human solid tumors.

## MATERIALS AND METHODS

### Patients and cohorts

We studied formalin-fixed paraffin-embedded (FFPE) primary stage I–IV NSCLCs from two retrospective cohorts, one from Yale University (cohort #1, n=329) and one from Greece (cohort #2, n=297) represented in tissue microarrays (TMAs).<sup>15</sup> A third cohort from Yale including advanced lung adenocarcinomas (LUADs) clinically tested for EGFR and KRAS mutations was also analyzed (cohort #3, n=182). Additionally, we analyzed 374 primary BCs represented in TMAs from two independent cohorts (cohorts #4 and #5). Cohort #4 included both ER<sup>+</sup> and ER<sup>−</sup> cases (n=235), and cohort #5 included only TNBCs (n=139). ER, PgR, and HER2 status was determined by the clinical laboratory and obtained from pathology reports. Detailed clinicopathologic characteristics of the cohorts are shown in the online supplemental tables S1 and S2. We also included baseline and on-treatment FFPE biopsy samples from three patients with stage IV TNBC treated for 2 weeks with the anti-SYK small molecule inhibitor TAK-659 after receiving three doses of nivolumab in the context of a phase I clinical trial (NCT02834247). The clinical outcome for these patients was progressive disease as best response.

### SYK antibody validation

To reliably detect SYK protein in FFPE tumor samples, we used a multimodal assay validation strategy of commercially available antibodies using multiplex immunofluorescence and immunoblots of positive and negative control preparations including morphologically normal human tissues, as well as unmodified and genetically engineered cell lines.

### Cell culture

Jurkat leukemia T cells, Ramos lymphoma B cells, A549 human lung adenocarcinoma (KRAS mutated) and H1975 adenocarcinoma (EGFR mutated) cell lines were purchased from ATCC and cultured in RPMI-1640 (1.8 g glucose/L) supplemented with 10% fetal calf serum and antibiotics (10,000 U/mL penicillin, 10  $\mu$ g/mL streptomycin) at 37°C and 5% CO<sub>2</sub>. Cell lines were authenticated every 3–6 months according to laboratory protocols.

### Western blot

Cell pellets were resuspended in 30–40  $\mu$ L of lysis buffer Tris Buffered Saline with Tween (TBST)/10% glycerol plus Halt Protease and Phosphatase Inhibitor Cocktail (Thermo Fisher). The cell pellet was incubated on ice for 40 min. After that, samples were spun at 14,000 rpm for 10 min at 4°C, and the supernatant was recovered. Protein quantification was performed using BioRad reagent, diluted 1:4 in miliQ H<sub>2</sub>O and measured using 600 nm optical density. Isolated protein in sample buffer was heated to 95°C for 10 min, and proteins were resolved on 4%–12% Bis–Tris gels (Invitrogen) at 100 V for 60 min. Proteins were transferred to nitrocellulose membranes using 1 $\times$  NuPage Transfer Buffer at 100 V for 1 hour. The membrane was blocked with 5% milk in 0.05% TBST at room temperature (RT) for 60 min and then incubated overnight at 4°C in blocking solution with 1:500 antibody dilution of anti-SYK (IgG2a-clone 4D10.1) or 1:1000 of anti-SYK (IgG1-clone SYK-01). Detection of  $\alpha$ -tubulin was conducted using a specific mouse monoclonal antibody diluted 1:5000 for 60 min at RT. Membranes were washed 3 $\times$  in 0.05% TBST and incubated with antimouse IgG, HRP-linked Antibody 1:5000 (Cell Signaling) for 60 min at RT. Detection of resolved protein was performed using Super Signal West Pico Chemiluminescent Substrate (Thermo Scientific), and images were recorded with the Image Lab V.4.1 software (Bio-Rad, USA).

### Quantitative immunofluorescence (QIF)

We constructed a custom TMA including positive (lymph node and tonsil) and negative (skeletal muscle and testis) control tissue samples. Histology sections from the TMA block were stained for SYK protein and other markers as indicated below using multiplex immunofluorescence.

### SYK downregulation using siRNA

Ramos cells were cultured in RPMI-1640 with 10% FBS, 1 mmol/L glutamine and 10 IU streptomycin/ampicillin and transferred to a medium containing low glucose DMEM 1% FBS 12 hours before transfection with SYK siRNAs. SYK knockdown was assayed using three distinct predesigned siRNAs (ID s13679, ID s13681 and ID s13680 from Ambion) or the mix of those three (siRNA SYKmix). Cells were transfected using 30 pmol Lipofectamin for 24 hours and then cultured with low glucose DMEM 1% FBS medium for additional 24 hours. Control unmodified and transfected cells were used for protein extraction and immunoblotting.

### In vitro cytokine treatment and flow cytometry analysis

Human A549 and H1975 cell lines were cultured in six-well plates until 70%–80% confluence. Cells were preincubated for 24 hours in serum-free RPMI-1640 medium and then exposed to recombinant TNF $\alpha$  (20–50–100 ng/mL) or IFN $\gamma$  (20–40–80 ng/mL) (R&D System, USA) for 24 hours in serum-free RPMI-1640. After treatments, cells were harvested, washed with PBS1 $\times$ /FCS 1% and fixed with Fixation buffer (Becton Dickinson, USA) for 30 min at 4°C. Cells were permeabilized with Perm/Wash buffer (Becton Dickinson, USA) for 15 min and stained with PE-anti-human SYK (IgG2a-clone 4D10.1) (eBioscience, California, USA) diluted in Perm/Wash buffer for 30 min at 4°C. Finally, the cells were washed twice in Perm/Wash buffer, acquired in a flow cytometer (Fortessa, BD) and results were analyzed using FCS Express V.6.0.

### In vitro alloreactive T cell stimulation

A549 and H1975 cells were left unstimulated or stimulated with TNF $\alpha$  (20 ng/mL), treated with the selective SYK/FLT3 inhibitor TAK-659 (25  $\mu$ M) (Takeda, Cambridge MA) or pretreated with TAK-659 for 10 min before adding TNF $\alpha$  for 24 hours in serum-free RPMI-1640. Cells were then recovered, washed in culture medium and analyzed by flow cytometry to determine the surface expression of HLA-ABC-FITC (BD, USA), CD86-PE (BD, USA), and FLT3-APC (BioLegend, USA). For intracellular staining, we used PE-antihuman SYK (eBioscience). A549 and H1975 cell lines were cocultured with allogeneic primary blood lymphocytes (PBLs) from healthy donors (ATCC) at different ratios 1:1–1:2–1:4–1:8–1:16 in flat-bottomed 96-well plates in serum-free AIM-V medium (Gibco BLR) for 18 hours and then analyzed for their expression of the early activation marker CD69-APC (BioLegend, San Diego, California, USA) in CD8-FITC (BD, USA). The mobilization of the degranulation marker CD107a in CD8<sup>+</sup> T cells was analyzed after 6 hours of coculture using a PE-conjugated antihuman-CD107a (BD, USA) and after incubation of the cell preparations for 1 hour with BD GolgiStop reagent (BD, USA). Finally, the cells were recovered and stained with FITC-antihuman CD8<sup>+</sup> and analyzed by flow cytometry.

### Immunoprofiling using targeted transcriptomics

Simultaneous and quantitative mRNA expression analysis of 770 individual immune related transcripts was conducted using the Nanostring Immune PanCancer assay. The experimental protocol was according to standard nCounter instructions and as previously reported by our group.<sup>16</sup> Cells were kept in control condition or treated with TAK-659, TNF $\alpha$  or TAK-659 plus TNF $\alpha$ . RNA extraction was performed using High Pure FFPE RNA isolation kit (Roche). Normalization of RNA scores was conducted using 40 Housekeeping Genes Reference to remove input variance and account for transcripts degradation.

### QIF panels

#### SYK panel

To selectively measure SYK in tumor, stromal and immune cells, we established a multiplexed QIF panel including primary antibodies anti-SYK (clone 4D10.1, Thermo Fisher; IgG2a 1:2500) targeting amino acid residues 313–339 of the full-length human SYK protein, CD45 (clone 2B11+PD7/26, Dako; IgG1 1:100) and pan cytokeratin (clone AE1/AE3, eBioscience, 1:100). TMA sections were deparaffinized and subjected to antigen retrieval with EDTA buffer (pH 8.0) for 20 min at 97°C in a pressure-boiling container, and blocking was performed with 0.3% BSA in 0.05% Tween solution for 30 min. Secondary antibodies conjugated to horseradish peroxidases (HRPs) specific to each primary antibody isotype and fluorescent reagents were used; antimouse IgG1 antibody (1:100, eBioscience) with Cy3-tyramide (Akoya) and antimouse IgG2a antibody (1:200, Abcam, Massachusetts, USA) with biotinylated tyramide/Streptavidin-Alexa750 conjugate (Akoya). Cytokeratin was detected with rabbit anti-pan cytokeratin-alexa 488-conjugated (Dako) diluted 1:100 in 0.3% BSA in 0.05% Tween solution for 60 min. Finally, nuclei were stained with DAPI. Residual HRP activity between incubations with secondary antibodies was eliminated by exposing the slides to a solution containing benzoic hydrazide (100 mmol/L) and hydrogen peroxide (50 mmol/L).

#### Tumor-infiltrating lymphocytes (TILs) panel

TILs were stained as described previously and using a validated immunofluorescence protocol.<sup>17</sup> Primary antibodies were incubated for 60 min at RT including anti-CD4 (SP35, Spring Bio, rabbit IgG 1:100), anti-CD8 (C8/144B, Dako, IgG1 1:250) and anti-CD20 (L26, Dako, IgG2a 1:150). Secondary antibodies were antirabbit IgG Envision (K4009, DAKO) with biotinylated tyramide/Streptavidin-Alexa750 conjugate (Akoya), antimouse IgG1 antibody (1:100, eBioscience) with Cy3-tyramide (Akoya), and antimouse IgG2a antibody (1:200, Abcam) with Cy5-tyramide (Akoya). Cytokeratin was detected with antirabbit pan cytokeratin (Dako) alexa488-conjugated diluted 1:100 in 0.3% BSA in 0.05% Tween solution for 60 min. Finally, nuclei were stained with DAPI.

#### Fluorescence measurement and scoring

Quantitative measurement of fluorescent signal for the different markers was performed using the AQUA method of QIF (Navigate Biopharma, USA). This algorithm allows for objective and accurate measurement of protein expression using marker-based signal colocalization.<sup>17</sup> The fluorescence scores obtained are normalized by the exposure time and bit depth, making them comparable across cases.

### Analysis of TCGA cohort DNA and RNA sequencing data

#### Clinical and molecular data

Data was obtained from the TCGA Research Network (<https://portal.gdc.cancer.gov/>). One thousand and

eleven lung cancer cases with available DNA and RNA-sequencing datasets were obtained for this analysis, 513 of them were lung adenocarcinomas (LUADs), and 498 were lung squamous cell carcinomas (LUSCs). For these patients, we collected their clinical profiles, whole exome sequencing bam files, somatic variants, and RNA-seq data.

#### Calculation of candidate HLA class I neoantigens and inflammation markers

To determine the candidate MHC class I neoantigen load, the whole exome sequencing bam files were used for MHC typing using POLYSOLVER.<sup>18</sup> The 8-11-mer mutant-containing neopeptides were generated by in silico frameshifting, and their binding affinities to host MHC-I were calculated using netMHCpan-4.0.<sup>19</sup> We used rank threshold smaller than 0.5 for neoantigen candidates filtering, per suggestion from the official netMHCpan instruction.<sup>20</sup> After quality control and results filtering, we obtained reliable HLA types and predicted MHC class-I neoantigen loads for 719 of the 1011 lung cancer samples. RNA-seq data was normalized in fragments per kilobase million to represent gene expression. Patients were divided into high/low SYK groups using the median SYK level as cut-off. The expression levels of CD4, CD8A, CTLA4, PD-L1, and MS4A1 were also studied.

#### Statistical analysis

Patient characteristics and differences between experimental groups were compared using t-test for continuous variables and  $\chi^2$  test for categorical variables. Relationships between continuous scores were analyzed using linear correlation coefficients. Overall survival (OS) functions between patients with high and low SYK were compared using log-rank test. Multivariate Cox proportional models were built to examine the effect of SYK on OS adjusted by the effect of stage, histology, and TILs. Survival analysis was performed by Mantel-Cox/log-rank test. SPSS V.19 statistical software was used.

## RESULTS

### Specific detection of SYK isoforms in human tissue samples

Limited performance of antibodies is a common issue affecting quality and reproducibility in scientific literature,<sup>21,22</sup> and therefore, validation of an assay to reliably detect human SYK in FFPE tumor samples was critical. The validation and optimization of an anti-SYK monoclonal antibody was performed using multiple steps including: (1) multiplexed QIF to stain positive/negative human control FFPE tissue specimens (online supplemental figures S1A,B), (2) comparison of results using two different SYK antibodies IgG2a-clone 4D10.1 (Thermo Fisher) and IgG1-clone SYK-01 (Thermo Fisher) (online supplemental figure S1C), (e) titrating the antibody to achieve optimal signal-to-noise ratio (online supplemental figure S1D); and (4) using western blot analysis of cell lines with and without targeted siRNA-based SYK downregulation. Western blots identified two bands, one

of 72kDa (L) and another of 50kDa (S) representing the two isoforms in positive Ramos cells, but not in the negative control Jurkat cells (online supplemental figure S1E,F).<sup>7</sup> Together, these results demonstrate the capacity of the assay to accurately measure both SYK protein isoforms in tumor biopsy samples.

### SYK expression in NSCLC

To determine the levels and tissue distribution of SYK in NSCLC, we used QIF panels for simultaneous and localized detection of DAPI for all cells, SYK protein, cytokeratin (CK) for tumor epithelial cells and CD45 for immune cells/leukocytes in 626 primary NSCLCs from two independent cohorts. SYK protein was detected in both tumor cells and leukocytes with cytoplasmic and nuclear staining pattern (figure 1A–B). However, there was a wide range with cases lacking detectable expression and a fraction showing high levels. Using the visual detection threshold obtained from positive and negative control samples as stratification cut-point (online supplemental figure S1), SYK protein was identified in 76% and 85% of cases in each cohort, respectively. The levels of SYK showed a continuous distribution across cases and a trend toward higher expression in CK-positive tumor cells than in CK-negative stromal cells or CD45+ leukocytes (figure 1C–D). In both cohorts, there was a positive association between SYK levels in different tumor tissue cells/compartments, suggesting a common mechanism driving SYK expression across them (figure 1E–H).

### SYK expression, tumor immune microenvironment and clinicopathologic associations in NSCLC

To study the relationship between SYK levels and major TIL subsets in NSCLC, we performed simultaneous measurement of DAPI, CK, CD4, CD8 and CD20 using QIF in consecutive sections from the cohorts. As expected, TILs were detected predominantly in the CK-negative stromal tissue compartment and focally infiltrating CK+ tumor cell nests (figure 1G–H). Elevated SYK protein in CK-positive tumor cells or CD45-positive leukocytes was significantly associated with higher CD4+ and CD8+ T cells, and this was consistent in both NSCLC cohorts (figure 1I–L and online supplemental tables S3-4). The association between SYK expression and the presence of CD20+ tumor infiltrating B-lymphocytes was inconsistent across cohorts, which could be due to the heterogeneous distribution of B cells typically forming tertiary lymphoid structures. As shown in online supplemental tables S3-4, we did not find consistent associations between SYK expression and age, gender, tumor histology variant, clinical stage and smoking status in both NSCLC cohorts.

To further assess the association between SYK and the tumor immune contexture in NSCLC, we performed analysis of LUAD and LUSC from The Cancer Genome Atlas (TCGA) cohort using bulk RNA sequencing. We found a positive association between elevated expression of SYK mRNA levels and CD8 $\alpha$ -chain (CD8A), CD4 and MS4A1 (CD20) transcripts in both lung tumor histology subsets

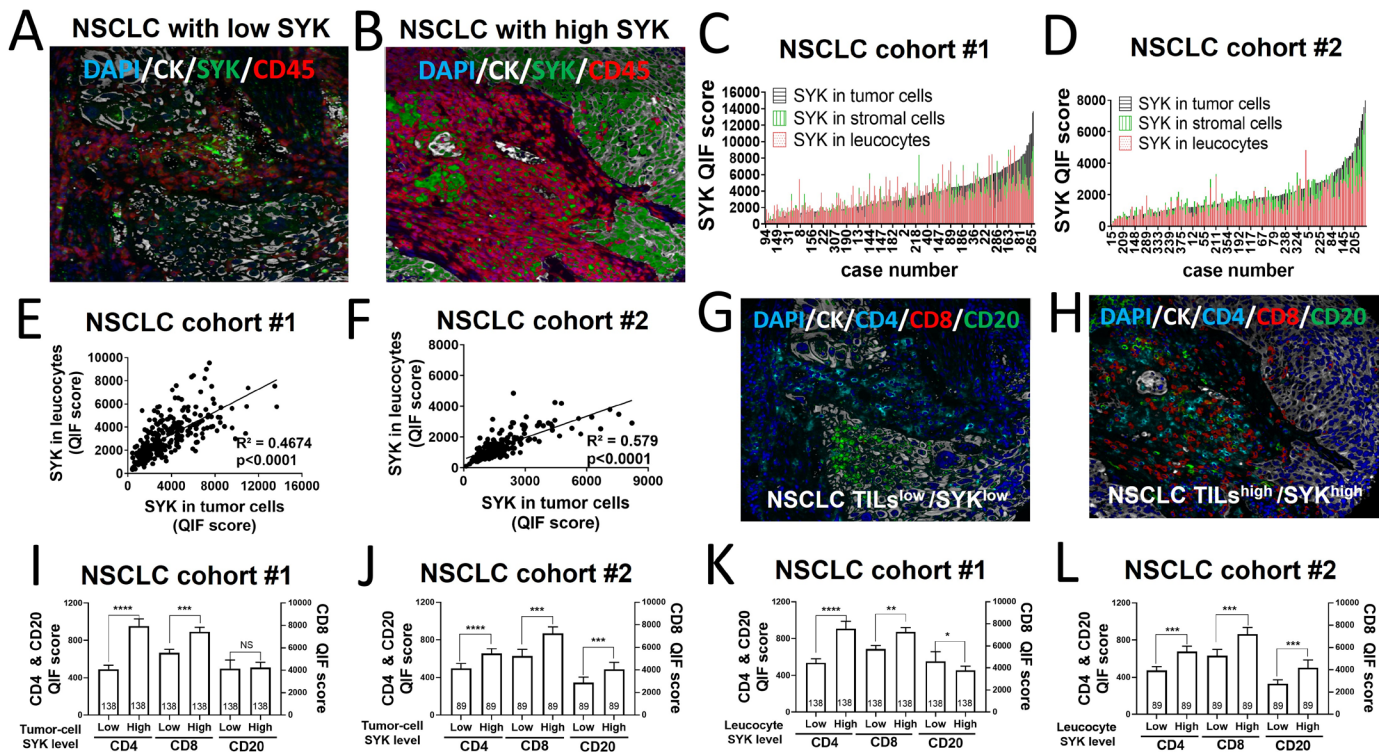


**Figure 1** SYK is expressed in a fraction of NSCLCs and is associated with increased TILs. (A and B) QIF images showing the simultaneous and localized detection of DAPI for all cells, SYK protein, cytokeratin (CK) for tumor epithelial cells and CD45 for immune cells in NSCLCs. (C and D) Distribution of SYK expression in specific tumor tissue compartments in two NSCLC cohorts (cohort #1 and cohort #2). (E and F) Correlation between SYK protein levels in CK+ tumor cells and CD45+ leukocytes. (G and H) QIF images showing the simultaneous staining of DAPI, CK, CD4, CD8 and CD20 in NSCLC. (I–L) Association between the SYK expression in tumor cells (land J) or leukocytes (K and L) and major TIL subsets in two independent NSCLC cohorts. The number of cases included in each analysis is indicated within each bar.  $R^2$ =linear regression coefficient. \* $P$ <0.05; \*\* $p$ <0.01; \*\*\* $p$ <0.001; \*\*\*\* $p$ <0.0001. NSCLCs, non-small cell lung carcinomas; QIF, quantitative immunofluorescence; SYK, spleen tyrosine kinase; TILs, tumor-infiltrating lymphocytes.

(figure 2A–F). We also observed a significant association between high SYK and elevated PD-L1 (figure 2G–H), further supporting a link between SYK in the tumor and adaptive anti-tumor responses in NSCLC. LUADs from TCGA with elevated SYK expression had lower tumor mutational burden and predicted HLA class-I neoantigens, but this was not seen in squamous malignancies (figure 2I–J). The prominent associations seen between SYK expression and major TIL subsets suggested a role of SYK in attracting or retaining TILs in the tumor microenvironment.

### SYK expression and dominant oncogenic driver mutations in NSCLC

To assess the expression of SYK in tumors with distinct and clinically relevant genomic alterations, we used QIF to analyze a retrospective collection of 149 LUADs with clinically tested activating KRAS and EGFR mutations (cohort #3). The levels of SYK in CK-positive tumor cells were significantly higher in EGFR and KRAS mutated tumors than in adenocarcinomas lacking mutations in both oncogenes (figure 2K). However, this difference was not detected when comparing the levels of SYK in CD45+ leukocytes (figure 2L), indicating a specific association

between SYK upregulation within the tumor cells and the presence of dominant oncogenic driver mutations.

### SYK expression and survival in NSCLC

To assess the biological and clinical significance of SYK expression in NSCLC, we determined the association between localized SYK levels in the cohorts and patient outcomes. Elevated expression of SYK in CK-positive tumor cells (above the median of the cohort) was prominently associated with longer 5-year OS, and this was consistent in both independent NSCLC cohorts (figure 3A–B). Notably, the survival effect of SYK expression measured in CK-negative stromal cells or CD45-positive tumor infiltrating leukocytes was less marked and non-statistically significant (figure 3C–F).

In a multivariate proportional hazards model including age, clinical stage, histology, smoking status and TIL levels as covariates, elevated tumor cell SYK was independently associated with longer survival in both collections (HR=0.49 and 0.45 ( $p$ <0.01), respectively, figure 3G–H). To explore the possible contribution of the L and S SYK splicing isoforms in the survival effect, we included in the Cox models the nuclear and cytoplasmic-specific tumor cell SYK levels. As shown in figure 3G–H, only the cytoplasmic SYK expression in CK+

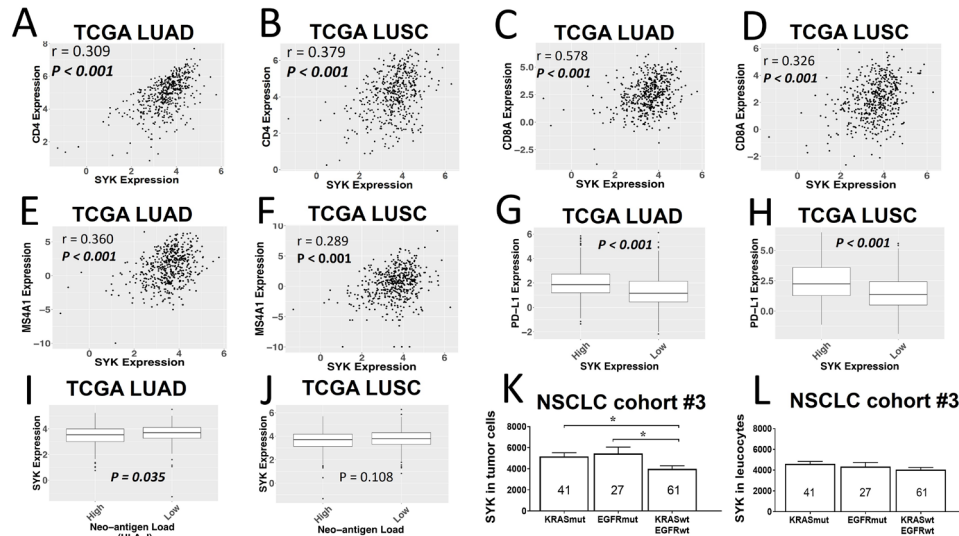


**Figure 2** SYK expression, immune associations and genomic features in lung adenocarcinomas (LUADs) and lung squamous cell carcinomas (LUSCs). (A–F) Association between SYK mRNA expression and CD4, CD8  $\alpha$ -chain (CD8A) and MS4A1 (CD20) transcripts in 513 LUADs and 498 LUSCs from the TCGA dataset. (G and H) Association between SYK and PD-L1 mRNA expression in LUADs and LUSCs from TCGA. (I and J) Association between SYK expression and the number of predicted HLA class-I tumor neoantigens in LUADs and LUSCs from TCGA. (K and L) Localized measurement of SYK by QIF in a retrospective collection of 149 LUADs clinically tested KRAS and EGFR mutations (cohort # 3). SYK levels were quantified in CK+ tumor cells (K) and in CD45+ leukocytes (L). The number of cases included in each analysis is indicated within each bar. R=Spearman's correlation coefficient. \* $P < 0.05$ . QIF, quantitative immunofluorescence; SYK, spleen tyrosine kinase; TCGA, The Cancer Genome Atlas.

tumor cells, but not the nuclear tumor cell fraction was independently associated with OS, supporting a dominant role of SYK(S) in the observed responses. Other variables with prominent survival effect were clinical disease stage and CD8+ T cell infiltration.

### Modulation of SYK by proinflammatory cytokines

To explore possible mechanisms mediating the association between SYK, tumor immune infiltration and favorable outcomes, we hypothesized that local production of proinflammatory cytokines by antitumor TILs could

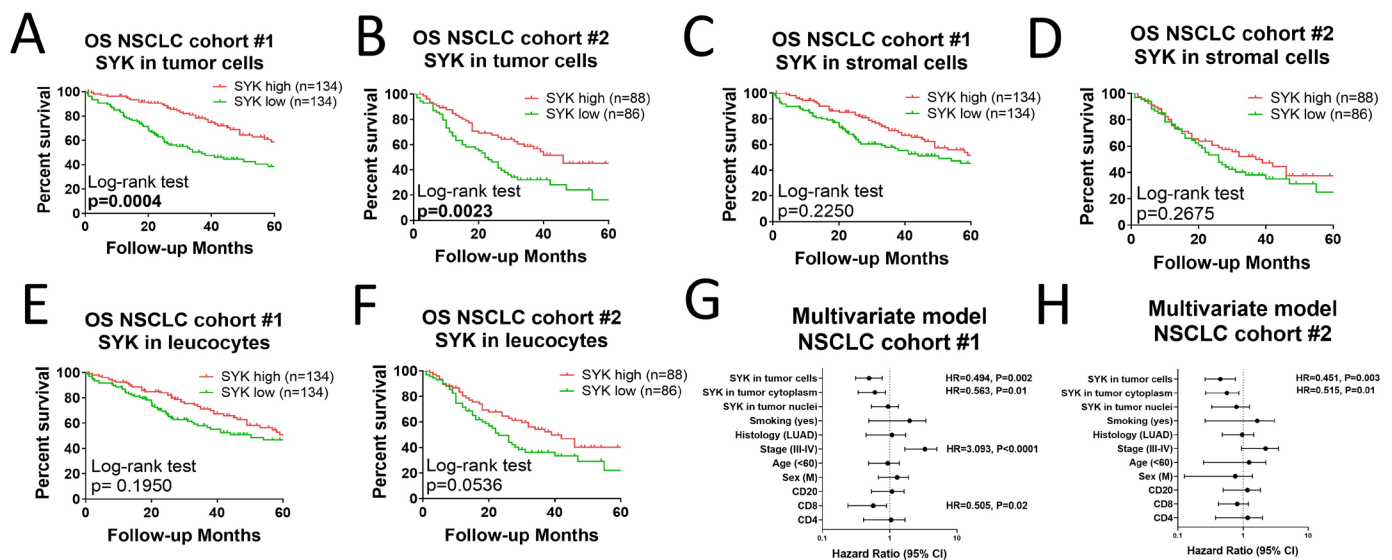


**Figure 3** Association between SYK levels and overall survival in NSCLC. (A–F) Kaplan–Meier graphical analysis of the 5-year overall survival in NSCLC cases from cohort #1 and cohort #2 based on the levels of SYK protein expression in the tumor cells (A and B), stromal cells (C and D) and CD45+ leukocytes (E and F). Cases were stratified by SYK QIF score (low vs high expression) using the median as a cut-off point. P values comparing risk groups were calculated with the log-rank test. (G and H) Forest plots showing the survival effect of localized SYK expression, TILs and major clinicopathologic variables in NSCLC cohorts. NSCLC, non-small cell lung carcinomas; SYK, spleen tyrosine kinase; TILs, tumor-infiltrating lymphocytes.

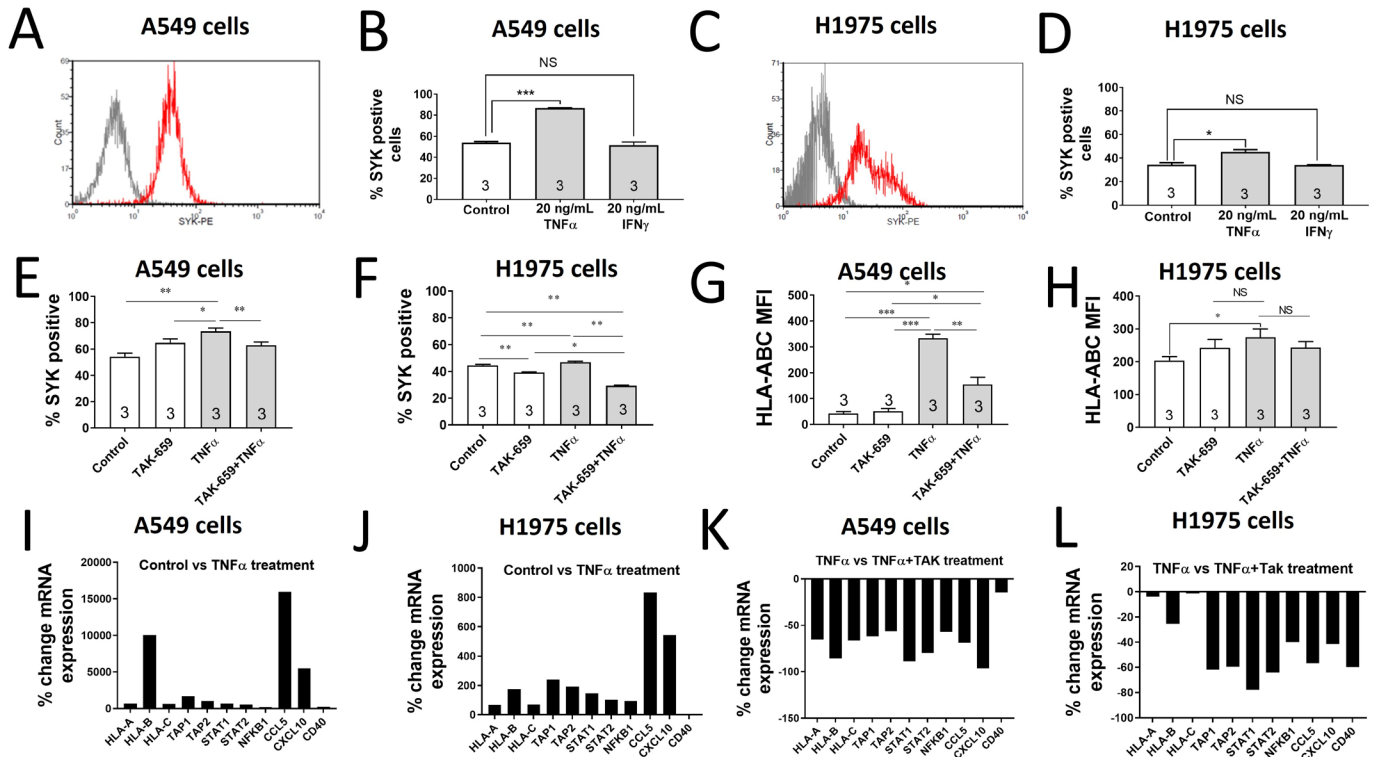


**Figure 4** TNF $\alpha$  induces SYK expression in lung cancer cells and SYK mediates proinflammatory responses. (A–D) SYK protein expression measured by flow cytometry in human lung cancer cell lines A549 (KRAS mutated) and H1975 (EGFR mutated) in vitro stimulated with human recombinant TNF $\alpha$  or IFN $\gamma$  for 24 hours. Panels A and C show histograms displaying the difference in the signal intensity obtained using isotype control staining (gray line) and anti-SYK PE-conjugated antibody (red line). (E–H) A549 and H1975 cell lines were left in control condition (medium) or treated with TNF $\alpha$ , TAK-659 or TAK-659 plus TNF $\alpha$  for 24 hours. After that, cells were recovered, stained with antibodies against SYK-PE (E and F), HLA-ABC-FITC (G and H) and analyzed by flow cytometry. (I–L) A549 and H1975 cells lines were treated with TAK659, TNF $\alpha$  alone or the combination for 24 hours. After that, samples were digested and total RNA was obtained using a high pure RNA isolation kit and transcript were analyzed using the NanoString platform targeted mRNA expression of 770 immune-related transcripts. The number of cases included in each analysis is indicated within each bar. \* $P < 0.05$ ; \*\* $p < 0.01$ . SYK, spleen tyrosine kinase.

mediate SYK upregulation in cancer cells. To test this, we identified two human LUAD cell lines with baseline SYK expression by flow cytometry, A549 (KRAS mutated) and H1975 (EGFR mutated). As shown in [figure 4A–D](#), treatment with 20 ng/mL human recombinant TNF $\alpha$  but not IFN $\gamma$  significantly increased SYK positivity in both lung cancer cell lines. The effect was not dependent on a specific concentration since a comparable effect was seen using different cytokine levels. The TNF $\alpha$ -induced increase in SYK protein expression was blocked by the small molecule inhibitor TAK-659,<sup>23</sup> a potent dual SYK/FLT3 inhibitor ([figure 4E–F](#)). Treatment with TAK-659 also suppressed the TNF $\alpha$ -dependent upregulation of HLA-ABC, supporting the requirement of SYK to mediate HLA class I protein upregulation in tumor cells. FLT3 protein was not detected in control or TNF $\alpha$ -treated A549 and H1975 cells, excluding its possible involvement in the observed responses (online supplemental figure S2).

To further assess the role of tumor cell SYK in the TNF $\alpha$ -dependent proinflammatory effect, we evaluated the expression of additional targets using targeted mRNA immunoprofiling of tumor cells before and after treatment. As shown in [figure 4I–J](#) and consistent with

its proinflammatory role, treatment of cultured lung tumor cells with TNF $\alpha$  upregulated markers involved in HLA class I antigen expression (HLA-A, HLA-B, HLA-C, TAP1 and TAP2), intracellular proinflammatory signals (STAT1, STAT2 and NFKB1), potent TILs chemoattractants (CCL5 and CXCL10) and the costimulatory receptor CD40. Treatment of cells with TAK-659 suppressed the proinflammatory changes induced by TNF $\alpha$ , and the effect was similar in A549 and H1975 cells ([figure 4K–L](#)).

The immunoregulatory effect of SYK blockade on lung tumor cells exposed to TNF $\alpha$  was not restricted to these targets and had a global impact in the expression of proinflammatory signals such as LTB $_4$ , CCL20, IL32 and CCL2 ([figure 5A–H](#)). In addition, SYK blockade induced changes in other genes potentially associated with TIL activation and antitumor immune responses including TNRSF17, IL10RA, LCK, GZMM and LAIR2. The top changed genes after treatment with TNF $\alpha$  or TNF $\alpha$  plus TAK-659 in A549 and H1975 cells are shown in [figure 5B, D, F and H](#).

To explore the functional impact of SYK in adaptive antitumor immune responses, we evaluated the effect of TAK-659 on T cell activation in cocultures of control

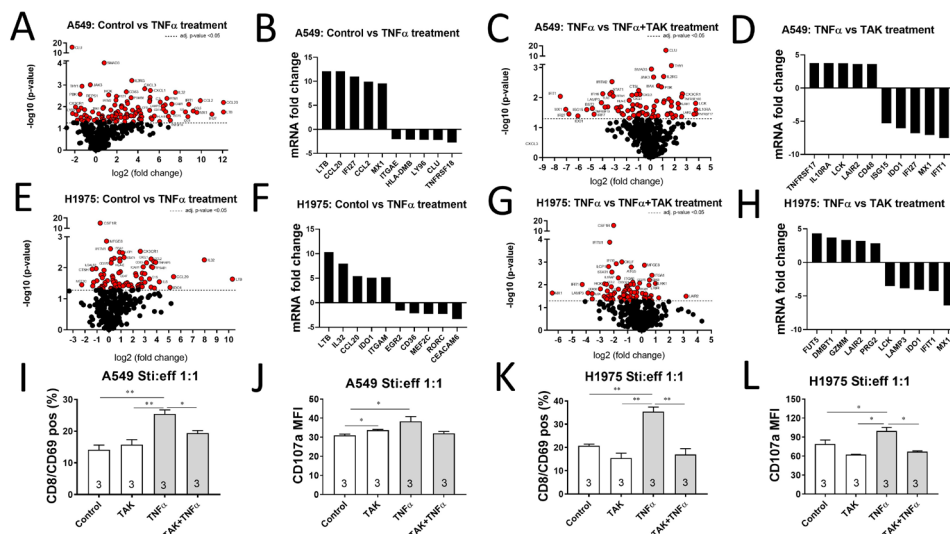


**Figure 5** Immune transcriptomic profiles and T cell responses against A549 or H1975 cells treated with TAK-659 and TNF $\alpha$ . (A–H) Targeted immune transcriptomic analysis of A549 and H1975 cells treated with TAK-659, TNF $\alpha$  alone or combination of both. Top changed transcripts are shown in bar charts. (I–L) A549 and H1975 cells were left in control condition (medium), treated with TNF $\alpha$ , TAK-659 or TAK-659 plus TNF $\alpha$  for 24 hours. After that, cells were recovered and cocultured at 1:1 ratio with allogeneic T cells for 6 hours (for CD107a staining) or 24 hours (for CD69 staining). Finally, T cells were double stained with anti-CD8-FITC/CD69-APC and CD8-FITC/CD107a-PE and analyzed by flow cytometry. \* $P < 0.05$ ; \*\* $p < 0.01$ .

or TNF $\alpha$  pretreated A549 or H1975 cells with allogeneic PBLs. As shown in [figure 5I–L](#), TAK-659 had no effect on control/untreated cell preparations but prevented the increase in the early activation marker CD69 on CD8+ effector cells when cocultured with tumor cells pretreated for 24 hours with TNF $\alpha$  before the addition of PBLs. Similarly, TAK-659 suppressed the TNF $\alpha$  mediated increase in the mobilization of the cytotoxic degranulation marker CD107a (LAMP1) in CD8+ effector cells and enhanced tumor cell apoptosis and cell death detected using Annexin V staining and 7-ADD, respectively (online supplemental figure S2). This suggests a direct effect of TAK-659 on tumor cells. In the latter experiments, TNF $\alpha$  was removed before addition of PBLs to rule out a direct effect on T cells. Together, these results reveal a prominent immunomodulatory role of SYK in anticancer T cell responses.

### SYK expression is associated with increased TILs and a triple negative phenotype in human breast cancer

To assess if the associations seen in NSCLC were generalizable to other tumor types, we evaluated the expression of SYK and major TIL subsets in BC. Breast malignancies are considered to be less T cell inflamed than lung tumors. We studied 374 primary BCs from two independent cohorts (cohorts #4 and #5). As shown in [figure 6A–B](#), SYK protein showed continuous distribution across breast malignancies with comparable levels in tumor and stromal/immune cells. SYK expression in CK-positive epithelial tumor cells was positively associated with CD4+ T cells in both cohorts, but the association with CD8+ and CD20+ TILs was inconsistent across the BC collections ([figure 6C–D](#)). In addition, elevated SYK protein was consistently associated with lack of estrogen receptor

(ER), progesterone receptor (PgR) and HER2 protein in BCs ([figure 6E–F](#)). Overall, the levels of SYK protein were lower in BC than in NSCLC in both tumor and immune cell compartments ([figure 6G–H](#)), and elevated SYK showed a non-significant trend toward better survival in breast malignancies that was more prominent in TNBCs from cohort #5 ([figure 6I–L](#)).

### Immunomodulatory effect of SYK in patients with cancer

To determine the local immunomodulatory effect of SYK *in vivo*, we analyzed the levels of TILs (DAPI/CK/CD8/CD4/CD20) and cell activation/proliferation (DAPI/CK/CD3/Granzyme-B/Ki-67) using QIF in baseline and post-treatment samples from three patients with advanced TNBC in a phase Ib clinical trial to evaluate TAK-659 in combination with nivolumab in patients with advanced solid tumors (NCT02834247). As shown in [figure 7A–F](#), SYK blockade induced significantly lower levels of CD3+, CD4+ and CD20+ TILs, as well as a mild (non-significant) reduction in CD8+ effector T cells ([figure 7E](#)). Blockade of SYK was also associated with decreased levels of CD3+ T cells, T cell Ki-67 levels and unchanged T cell granzyme-B ([figure 7F](#)). Together, these results evidence a negative local immunomodulatory effect of SYK blockade in patients with TNBC.

### DISCUSSION

The expression of SYK in cancer cells has been associated with both tumor promoting and tumor suppressive effects. However, the role of tumor cell SYK in adaptive anticancer immune responses remained poorly understood. Here, we show that SYK protein expression in the tumor is associated with favorable T cell responses



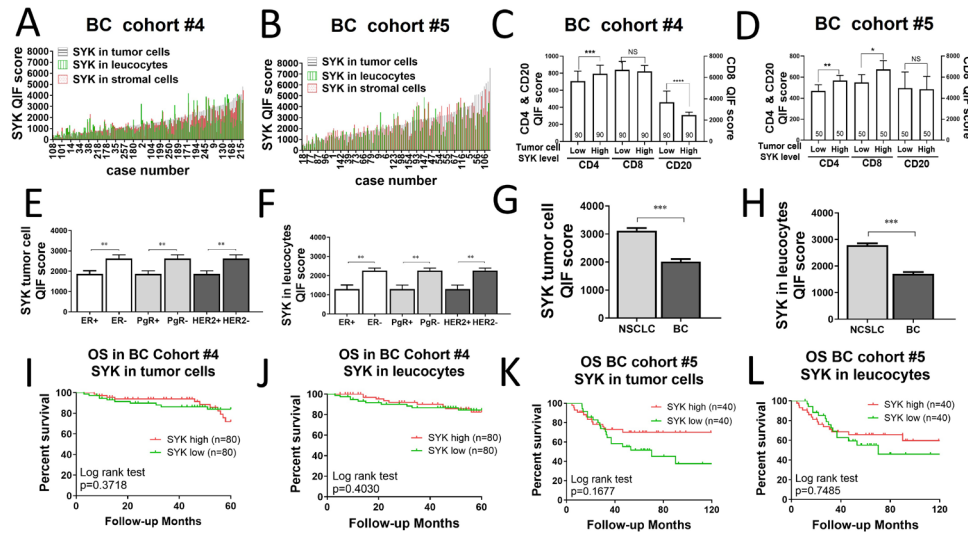


**Figure 6** Expression of SYK in breast cancer (BC). (A and B) Quantification and distribution of SYK protein levels in BC by quantitative fluorescence (QIF). SYK protein expression in cases from cohort #4 and cohort #5 (TNBC) selectively measured in tumor, stroma and CD45+ leukocytes. (C and D) Association between tumor cell SYK levels and major TIL subsets in BC. (E and F) Association between tumor cell SYK protein levels and hormone receptor expression or HER2 status in BC. (G and H) Comparative analysis of SYK protein levels in NSCLC and BC cohorts. (I–L) Kaplan–Meier graphical analysis of the 5-year overall survival in BC cases from cohort #3 and cohort #4 based on the levels of SYK protein expression in the tumor cells or in CD45+ leukocytes. The number of cases included in each analysis is indicated within each bar. \* $P < 0.05$ ; \*\* $p < 0.01$ . \*\*\* $p < 0.001$ . NSCLC, non-small cell lung carcinoma; SYK, spleen tyrosine kinase; TNBC, triple negative breast cancer.

and better outcome in human lung and breast malignancies. We also show that tumor cell SYK expression is induced by  $TNF\alpha$ , has a prominent immunomodulatory effect in vitro and in vivo, and mediates proinflammatory responses induced by this cytokine.

Revealing the role of SYK in cancer has been limited by literature discordances probably reflecting its context-dependent and tumor-type specific functions. In acute myeloid leukemia, high phosphorylated SYK expression is associated with unfavorable outcome independent of age, cytogenetics, and white blood cell count.<sup>24</sup> SYK elicits a prosurvival signal in lymphoid malignancies and non-immune cells but can also suppress tumorigenesis by restricting epithelial-mesenchymal transition, enhancing cell–cell interactions, and inhibiting cell migration.<sup>5</sup> Pharmacological inhibition or genetic silencing of SYK induces antitumor responses in models of diverse tumor types such as leukemia/lymphoma, retinoblastoma, ovarian carcinomas, small cell lung cancer and squamous head and neck malignancies.<sup>5</sup> However, induction of SYK expression has also been shown to increase the cell adhesion and decrease tumor cell migration and invasion.<sup>10</sup> Consistent with this notion, loss of SYK expression has been correlated with poor survival and the presence of tumor metastasis in patients with liver, pancreas, bladder, breast, and gastric cancer.<sup>25–29</sup> Unfortunately, most of the aforementioned studies were conducted using qualitative methods and were not able to distinguish between SYK expression on specific cell populations or compartments. In addition, these studies did not address or considered the role of SYK in modulating adaptive antitumor responses.

Our results confirm that elevated expression of SYK protein is associated with better survival in NSCLC and BC. Moreover, our results reveal that SYK expression in tumor cells, and in particular of the cytoplasmic SYK(S) isoform, is an independent prognostic marker. The independence of the survival effect of tumor cell SYK expression from T cell infiltration in multivariate models supports a tumor-intrinsic mechanism involved in this effect. Future studies will be required to determine if SYK expression in tumors can predict sensitivity or resistance to specific anticancer treatments.

To our knowledge, our study is the first to demonstrate a T cell immunomodulatory role of SYK expression in human solid tumors. A previous study reported that macrophage SYK expression drives alternative polarization of immunosuppressive tumor-associated macrophages in syngeneic LLC lung and B16 melanoma mouse tumor models.<sup>14</sup> In this study, selective SYK deletion in macrophages or systemic SYK inhibition using Fostamatinib/R406 induced favorable myeloid cell polarization, reduced tumor growth/metastases and increased the levels of proinflammatory cytokines and CD8+ T cell responses. This led to propose SYK blockade as an immunostimulatory anticancer drug candidate. However, LLC and B16 melanoma cells do not express detectable levels of SYK, which could at least partially explain the apparent differences with our findings using human cells and tumors. In addition, our work did not analyze the responses selectively in tumor-associated macrophages.

An intriguing finding of our study was the increased expression of SYK in LUADs harboring lower tumor mutational burden and candidate HLA class I neoantigens

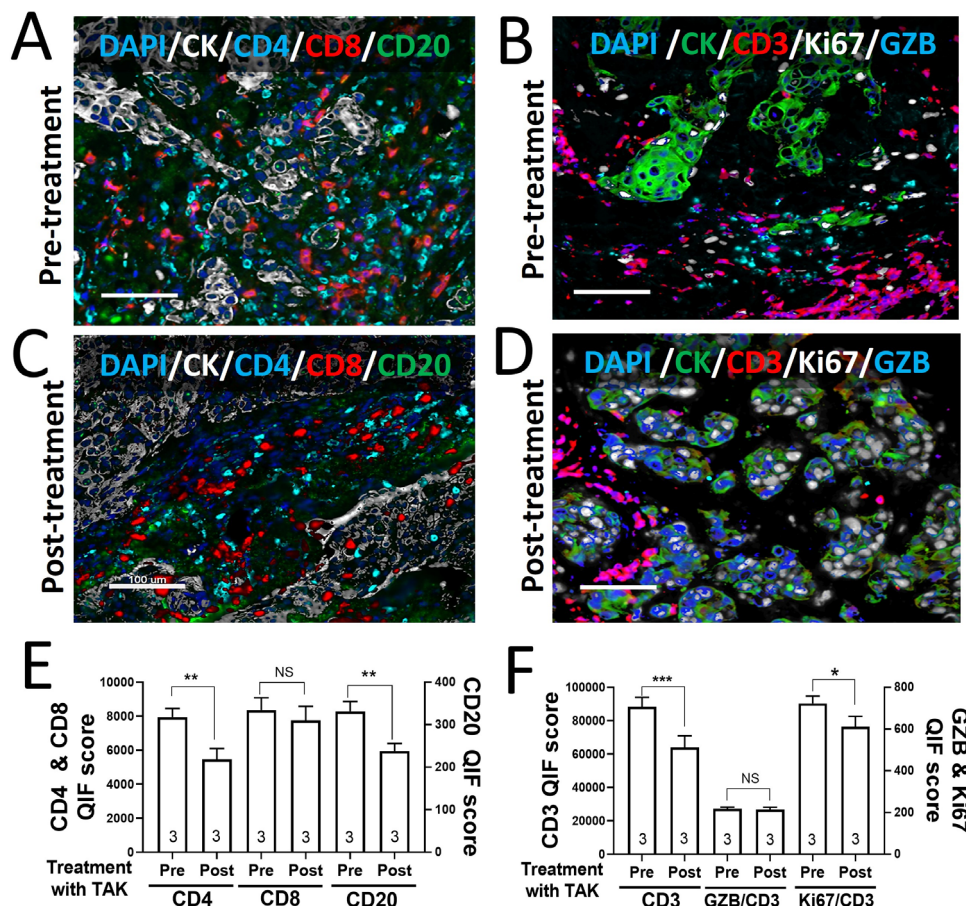


**Figure 7** Immunomodulatory effect of SYK in patients with breast cancer treated with the SYK inhibitor TAK-659. (A–C) QIF analysis of TILs (CD8/CD4/CD20/CK/DAPI) and T cell activation/proliferation (CD3/granzyme-B/Ki-67/CK/DAPI) in baseline (pre) and post-treatment samples (post) from three consecutive patients with advanced triple negative breast cancer treated for 2 weeks with TAK-659 in a phase I clinical trial (NCT02834247). (E and F) Quantification of the markers in baseline and post-treatment tumor samples. The number of cases included in each analysis is indicated within each bar. \* $P < 0.05$ . QIF, quantitative immunofluorescence; SYK, spleen tyrosine kinase; TILs, tumor-infiltrating lymphocytes.

and with activating mutations in EGFR and KRAS. A previous study using siRNA-based screens identified SYK as the most differentially expressed kinase between KRAS-mutant/dependent and KRAS wild-type lung and pancreatic human carcinoma cells.<sup>30</sup> Moreover, ablation of KRAS reduced SYK protein levels and targeted SYK deletion or competitive inhibition with R406 resulted in loss of epithelial cell features and caspase-3 dependent cell death in KRAS-dependent tumor cells. These results suggested SYK blockade as a possible therapeutic option to treat KRAS addicted cancers. Our findings of increased tumor cell apoptosis/death after SYK blockade using TAK-659 in both KRAS and EGFR mutant LUAD cell lines are consistent with this interpretation (online supplemental figure S2). However, the direct antitumor effect of SYK inhibition could be counteracted by suppression of favorable immunomodulatory responses in the tumor microenvironment to ultimately limit tumor rejection. This is also supported by the lack of antitumor activity seen in patients with TNBC treated with TAK-659 and PD-1 blockade in a phase I clinical trial, all of which showed progressive disease as best response (NCT02834247). The results from the clinical trial including safety profile

and additional patients with other tumor types will be reported in a separate manuscript.

The prominent association between SYK expression and increased TILs in lung and breast carcinomas can be explained by the induction of SYK by TNF $\alpha$  produced by activated immune cells and the proinflammatory effect of TNF $\alpha$  on SYK expressing tumor cells that can promote and amplify the adaptive antitumor immune responses. Therefore, tumor cell SYK expression can be both a sensor and promoter of T cell infiltration in lung and breast malignancies. The downregulation of SYK expression in cancer cells could limit the proinflammatory responses and antigen presentation capacity of tumor cells in response to cytokines and favor tumor immune evasion and resistance to immunostimulatory therapies.

Our study has limitations. First, the analysis of tumor tissues was conducted using TMAs from retrospectively collected tumor cases that may over or under-represent the markers levels. However, the relatively large number of cases analyzed and the use of multiple independent cohorts support the robustness of our findings. In addition, diverse reports from our group and others using TMAs have shown consistent results and significant association

with clinicopathologic variables and outcomes using this approach, supporting its reliability.<sup>17 20 31</sup> Another possible limitation is the inclusion of cases treated in a non-controlled fashion in the retrospective cohorts. This is a common limitation of retrospective studies and its possible impact on the results is uncertain. Future studies using syngeneic mouse models with orthotopic tumor engraftments or conditional/inducible knockout models will be required to carefully study the functional impact of SYK inhibition or genetic ablation in selected cell types such as myeloid cells. Finally, the studies of T cell functional profiles after cocultures of PBLs with tumor cells pretreated with SYK blocker were conducted using allogeneic (polyclonal) T cell recognition that may be more potent than endogenous antigen specific anti-tumor responses. However, the consistency of our results seen in vitro and in vivo on samples from patients treated with TAK-659 in a clinical trial supports the validity of our findings.

#### Author affiliations

<sup>1</sup>Department of Pathology, Yale School of Medicine, New Haven, Connecticut, USA

<sup>2</sup>Translational Medicine Laboratory, Department of Cancer Research, Instituto Oncologico Fundacion Arturo Lopez Perez, Santiago 8320000, Chile

<sup>3</sup>Yale School of Public Health, Yale University, New Haven, Connecticut, USA

<sup>4</sup>Department of Oncology, University of Athens, Athens, Greece

<sup>5</sup>Takeda Oncology, Cambridge, Massachusetts, USA

**Contributors** Study conception and design: AA-D and KAS; sample acquisition: AAD and NG; nanostring experiments and analysis: NG and KAS; tissue microarray design: KS; triple negative breast cancer samples: WLT, KK, and RCG; in vitro experiments: AAD and NG; Western blot experiments: AAD and SD; staining and image analysis: AAD and FV-E; statistical analyses: DT, HZ, AAD, and KAS; drafting of manuscript: KAS and AAD. Guarantor: KAS.

**Funding** Funded by a research grant from Takeda, NIH grants R03CA219603 (KAS), R37CA245154 (KAS), and R01CA262377 (KAS).

**Competing interests** KAS reports research funding from Navigate Biopharma, Tesaro/GlaxoSmithKline, Moderna Inc, Takeda, Surface Oncology, Pierre-Fabre Research Institute, Merck-Sharp & Dohme, Bristol-Myers Squibb, AstraZeneca, Ribon Therapeutics, Akoya Biosciences, Eli Lilly and Boehringer-Ingelheim. KAS has received honoraria for consultant/advisory/speaker roles from Moderna Inc, Shattuck Labs, Pierre-Fabre, AstraZeneca, EMD Serono, Ono Pharmaceuticals, Clinica Alemana de Santiago, Dynamo Therapeutics, PeerView, Abbvie, Fluidigm, Takeda/Millennium Pharmaceuticals, Merck-Sharp & Dohme, Bristol Myers-Squibb, Agenus, Parthenon Therapeutics, Molecular Templates, and Torque Therapeutics.

**Patient consent for publication** Not applicable.

**Ethics approval** This study involves human participants and was approved by Yale Human Investigation Committee protocol #1608018220. Participants gave informed consent to participate in the study before taking part.

**Provenance and peer review** Not commissioned; externally peer reviewed.

**Data availability statement** Data are available on reasonable request.

**Supplemental material** This content has been supplied by the author(s). It has not been vetted by BMJ Publishing Group Limited (BMJ) and may not have been peer-reviewed. Any opinions or recommendations discussed are solely those of the author(s) and are not endorsed by BMJ. BMJ disclaims all liability and responsibility arising from any reliance placed on the content. Where the content includes any translated material, BMJ does not warrant the accuracy and reliability of the translations (including but not limited to local regulations, clinical guidelines, terminology, drug names and drug dosages), and is not responsible for any error and/or omissions arising from translation and adaptation or otherwise.

**Open access** This is an open access article distributed in accordance with the Creative Commons Attribution Non Commercial (CC BY-NC 4.0) license, which permits others to distribute, remix, adapt, build upon this work non-commercially,

and license their derivative works on different terms, provided the original work is properly cited, appropriate credit is given, any changes made indicated, and the use is non-commercial. See <http://creativecommons.org/licenses/by-nc/4.0/>.

#### ORCID iDs

Franz Villarroel-Espindola <http://orcid.org/0000-0003-0080-2444>

Shruti Desai <http://orcid.org/0000-0002-5234-5890>

Kurt A Schalper <http://orcid.org/0000-0001-5692-4833>

#### REFERENCES

- Okkenhaug K, Vanhaesebroeck B. PI3K in lymphocyte development, differentiation and activation. *Nat Rev Immunol* 2003;3:317–30.
- Coopman PJ, Mueller SC. The Syk tyrosine kinase: a new negative regulator in tumor growth and progression. *Cancer Lett* 2006;241:159–73.
- Heizmann B, Reth M, Infantino S. Syk is a dual-specificity kinase that self-regulates the signal output from the B-cell antigen receptor. *Proc Natl Acad Sci U S A* 2010;107:18563–8.
- Yanagi S, Inatome R, Takano T, et al. Syk expression and novel function in a wide variety of tissues. *Biochem Biophys Res Commun* 2001;288:495–8.
- Krisenko MO, Geahlen RL. Calling in SYK: SYK's dual role as a tumor promoter and tumor suppressor in cancer. *Biochimica et Biophysica Acta (BBA) - Molecular Cell Research* 2015;1853:254–63.
- Prinos P, Garneau D, Lucier J-F, et al. Alternative splicing of Syk regulates mitosis and cell survival. *Nat Struct Mol Biol* 2011;18:673–9.
- Hong J, Yuan Y, Wang J, et al. Expression of variant isoforms of the tyrosine kinase Syk determines the prognosis of hepatocellular carcinoma. *Cancer Res* 2014;74:1845–56.
- Gao J, Aksoy BA, Dogrusoz U, et al. Integrative analysis of complex cancer genomics and clinical profiles using the cBioPortal. *Sci Signal* 2013;6:pl1.
- Gordon LI, Kaplan JB, Papat R, et al. Phase I study of TAK-659, an investigational, dual SYK/FLT3 inhibitor, in patients with B-cell lymphoma. *Clin Cancer Res* 2020;26:3546–56.
- Bailot O, Fenouille N, Abbe P, et al. Spleen tyrosine kinase functions as a tumor suppressor in melanoma cells by inducing senescence-like growth arrest. *Cancer Res* 2009;69:2748–56.
- Coopman PJ, Do MT, Barth M, et al. The Syk tyrosine kinase suppresses malignant growth of human breast cancer cells. *Nature* 2000;406:742–7.
- Fueyo J, Alonso MM, Parker Kerrigan BC, et al. Linking inflammation and cancer: the unexpected SYK world. *Neuro Oncol* 2018;20: :582–3.
- Moncayo G, Grzmil M, Smirnova T, et al. SYK inhibition blocks proliferation and migration of glioma cells and modifies the tumor microenvironment. *Neuro Oncol* 2018;20:621–31.
- Joshi S, Liu KX, Zulcic M, et al. Macrophage Syk-PI3Kγ inhibits antitumor immunity: SRX3207, a novel dual Syk-PI3K inhibitory chemotype relieves tumor immunosuppression. *Mol Cancer Ther* 2020;19:755–64.
- Villarroel-Espindola F, Yu X, Datar I, et al. Spatially resolved and quantitative analysis of VISTA/PD-1H as a novel immunotherapy target in human non-small cell lung cancer. *Clin Cancer Res* 2018;24:1562–73.
- Schalper KA, Rodriguez-Ruiz ME, Diez-Valle R, et al. Neoadjuvant nivolumab modifies the tumor immune microenvironment in resectable glioblastoma. *Nat Med* 2019;25:470–6.
- Schalper KA, Brown J, Carvajal-Hausdorf D, et al. Objective measurement and clinical significance of TILs in non-small cell lung cancer. *J Natl Cancer Inst* 2015;107. doi:10.1093/jnci/dju435. [Epub ahead of print: 03 02 2015].
- Shukla SA, Rooney MS, Rajasagi M, et al. Comprehensive analysis of cancer-associated somatic mutations in class I HLA genes. *Nat Biotechnol* 2015;33:1152–8.
- Jurtz V, Paul S, Andreatta M, et al. NetMHCpan-4.0: improved peptide-MHC class I interaction predictions integrating eluted ligand and peptide binding affinity data. *J Immunol* 2017;199:3360–8.
- Datar I, Sanmamed MF, Wang J, et al. Expression analysis and significance of PD-1, LAG-3, and Tim-3 in human non-small cell lung cancer using spatially resolved and multiparametric single-cell analysis. *Clin Cancer Res* 2019;25:4663–73.
- Uhlen M, Bandrowski A, Carr S, et al. A proposal for validation of antibodies. *Nat Methods* 2016;13:823–7.
- Voskuil JLA. The challenges with the validation of research antibodies. *F1000Res* 2017;6:161.



- 23 Lam B, Arikawa Y, Cramlett J, *et al.* Discovery of TAK-659 an orally available investigational inhibitor of spleen tyrosine kinase (Syk). *Bioorg Med Chem Lett* 2016;26:5947–50.
- 24 Boros K, Puissant A, Back M, *et al.* Increased Syk activity is associated with unfavorable outcome among patients with acute myeloid leukemia. *Oncotarget* 2015;6:25575–87.
- 25 Toyama T, Iwase H, Yamashita H, *et al.* Reduced expression of the Syk gene is correlated with poor prognosis in human breast cancer. *Cancer Lett* 2003;189:97–102.
- 26 Kunze E, Wendt M, Schlott T. Promoter hypermethylation of the 14-3-3 sigma, Syk and CAGE-1 genes is related to the various phenotypes of urinary bladder carcinomas and associated with progression of transitional cell carcinomas. *Int J Mol Med* 2006;18:547–57.
- 27 Layton T, Stalens C, Gunderson F, *et al.* Syk tyrosine kinase acts as a pancreatic adenocarcinoma tumor suppressor by regulating cellular growth and invasion. *Am J Pathol* 2009;175:2625–36.
- 28 Lee HS, Kim B-H, Cho N-Y, *et al.* Prognostic implications of and relationship between CpG island hypermethylation and repetitive DNA hypomethylation in hepatocellular carcinoma. *Clin Cancer Res* 2009;15:812–20.
- 29 Shin S-H, Lee KH, Kim B-H, *et al.* Downregulation of spleen tyrosine kinase in hepatocellular carcinoma by promoter CpG island hypermethylation and its potential role in carcinogenesis. *Lab Invest* 2014;94:1396–405.
- 30 Singh A, Greninger P, Rhodes D, *et al.* A gene expression signature associated with "K-Ras addiction" reveals regulators of EMT and tumor cell survival. *Cancer Cell* 2009;15:489–500.
- 31 Gettinger SN, Choi J, Mani N, *et al.* A dormant TIL phenotype defines non-small cell lung carcinomas sensitive to immune checkpoint blockers. *Nat Commun* 2018;9:3196.